The ROYAL COLLEGE of
OPHTHALMOLOGISTS

ARTICLE

Choroidal thickness and the retinal ganglion cell complex in chronic Leber's hereditary optic neuropathy: a prospective study using swept-source optical coherence tomography

Fatemeh Darvizeh[1,2] · Samuel Asanad [1,3] · Khalil Ghasemi Falavarjani [4] · Jessica Wu[3] · Jack J. Tian [1] ·
Francesco Bandello[2] · Fred N. Ross-Cisneros[1] · Piero Barboni[2] · Enrico Borrelli [2] · Alfredo A. Sadun[1,3]

Abstract

Background/Objectives Choroidal thinning has been suggested in Leber's hereditary optic neuropathy (LHON). No study has been conducted of the choroid in relation to the retinal ganglion cell-inner plexiform layer (RGC-IPL). We sought to measure choroidal thickness in chronic LHON and to correlate thickness changes with the RGC-IPL.
Subjects/Methods Chronic LHON, 11778 mitochondrial DNA (mtDNA) mutation, patients (26 eyes; mean age: 35.1 ± 16.1 years) were prospectively recruited at Doheny Eye Center, University of California Los Angeles from March 2016 to July 2017. Age-matched healthy controls (27 eyes; mean age: 32.4 ± 11.1 years) were enroled for comparison. Swept-source optical coherence tomography (SS-OCT) imaging was performed in chronic LHON patients and compared with age-matched healthy controls.
Results The macular choroid was significantly thinner in chronic LHON ($250.5 \pm 62.2\,\mu m$) compared with controls ($313.9 \pm 60.2\,\mu m$; $p < 0.0001$). The peripapillary choroid was also significantly thinner in chronic LHON ($135.7 \pm 51.4\,\mu m$) compared with controls ($183.0 \pm 61.8\,\mu m$, $p < 0.001$). Choroidal thickness strongly correlated with retinal nerve fibre layer (RNFL) thickness in both the macular ($R^2 = 0.72$; 95% CI, 0.57–0.84) and peripapillary regions ($R^2 = 0.53$; 95% CI, 0.31–0.70). Choroidal thickness was also significantly correlated with macular RGC-IPL thickness ($R^2 = 0.51$; 95% CI, 0.26–0.73).
Conclusions Choroidal thinning in chronic LHON correlated strongly with both RNFL and RGC-IPL thicknesses. These findings may suggest a pathophysiological mechanism involving vascular pathology of the choroid in relation to the retinal ganglion cell complex in LHON.

Introduction

Leber's hereditary optic neuropathy (LHON) is a rare, maternally inherited mitochondrial disease that may be characterized by bilateral loss of vision with a gender distribution

✉ Samuel Asanad
samuelasanad@gmail.com

1 Doheny Eye Institute, Los Angeles, CA, USA

2 Department of Ophthalmology, San Raffaele Scientific Institute, Milan, Italy

3 Department of Ophthalmology, David Geffen School of Medicine, University of California Los Angeles, Los Angeles, CA, USA

4 Eye Research Center, Rassoul Akram Hospital, Iran University of Medical Sciences, Tehran, Iran

ratio as high as 9:1 between males and females, respectively [1–4]. Three mitochondrial mutations at nucleotide positions m.11778G > A, m.3460G > A m.11484T > C result in defective subunit expression of complex I protein in the electron transport chain, and account for ~90% of LHON cases [4–8]. Characteristic patterns of retinal nerve fibre layer (RNFL) thickening from nerve fibre swelling in early or acute stages of LHON followed by RNFL thinning from decreased nerve fibre swelling in late or chronic stages of LHON have been observed [9–11]. Acute LHON has been characterized by significant nerve fibre thickening in the superior and inferior quadrants followed later by swelling of nasal fibres, while in chronic LHON there is differential preservation of the nasal nerve fibres [4–6].

Aside from these structural nerve fibre changes, optical coherence tomography (OCT) studies have also suggested vascular pathology in LHON. Our laboratory recently demonstrated that RNFL thickening in acute LHON is accompanied by choroidal thickening, and RNFL thinning

in chronic LHON is similarly accompanied by choroidal thinning [11]. This study also showed a direct correlation between RNFL and choroidal thicknesses in LHON, suggesting that RNFL thickness may be associated with changes in the choroid [11]. These findings suggest that while LHON has been shown to involve the retinal ganglion cells (RGCs) and their axons in the optic nerve [5, 6, 12, 13], a vascular aetiology may also be involved. More recent studies conducted by our group revealed that the macular RGC-inner plexiform layer (RGC-IPL) thickness changes may precede the wave of peripapillary RNFL swelling classically seen in acute LHON [14]. Given this earlier involvement, we proposed that the RGC-IPL might serve as a more sensitive marker for assessing and monitoring disease progression [14, 15]. These retinal and choroidal studies were predominantly performed using a spectral domain OCT (SD-OCT) device. Recent advances in ocular imaging with the introduction of swept-source OCT (SS-OCT) have enabled clinicians to visualize the retinal and choroidal structures with greater detail, resolution, and penetrance compared with previous OCT imaging modalities [16]. In the present study, we explored the relationship between inner retinal layer thicknesses, mainly RGC-IPL, and the choroid in chronic LHON using SS-OCT. We hypothesized that in the chronic disease stages of LHON, choroidal thickness would be significantly reduced and these thickness changes would correlate with that of the macular RGC-IPL and RNFL thickness.

Methods

Twenty-six LHON patients (mean age: 35.1 ± 16.1 years) with disease duration >12 months were recruited for the study at Doheny Eye Center, University of California Los Angeles (UCLA) from March 2016 to July 2017. The study was approved by the Institutional Review Board at UCLA. Informed consent was obtained from all subjects and the study was conducted in accordance with the Declaration of Helsinki.

All LHON subjects included in this study had a genetically confirmed diagnosis of LHON, 11778 mitochondrial DNA (mtDNA) mutation. Subjects with confounding retinal pathology, optic nerve disease besides LHON, or systemic conditions potentially affecting the vascular system (e.g. autoimmune condition, diabetes, and uncontrolled systemic hypertension) were excluded. All subjects underwent extensive ophthalmologic characterization, including best corrected visual acuity (BCVA) measurement with the Early Treatment Diabetic Retinopathy Study chart, expressed as a logarithm of the minimum angle of resolution (logMAR), slit-lamp biomicroscopy, intraocular pressure (IOP) measurement, and dilated fundus examination. For each LHON patient, images of both eyes were initially acquired. Given the symmetry of

disease and statistical indifference upon inclusion of both eyes in the analysis, we randomly selected and included only the right eye for analysis. Twenty-seven age-matched healthy controls (27 eyes) (mean age: 32.4 ± 11.1 years) were identified and enroled for comparison. Control subjects had normal ocular examination including an IOP lower than 20 mm Hg, BCVA of 0.0 logMAR with a refractive error between -3.00 and $+3.00$ spherical equivalent, no evidence of optic disk or retinal disease, or systemic conditions that may affect the vascular system (e.g. autoimmune condition, diabetes, and uncontrolled systemic hypertension).

Instrumentation and procedures

OCT images were taken using SS-OCT (DRI-OCT, Triton, Tokyo, Japan). The instrument uses a wavelength of 1050 nm with a scan speed of 100,000 A-scans per second. The images were obtained using a 3-dimensional (3D) wide scan protocol with a size of 12×9 mm consisting of 256 B-scans, each comprising 512 A-scans. This allowed obtaining images of the macular and optic nerve head region in a single scan. The total acquisition time was 1.3 s per 12×9 mm scan. Following proper seating and alignment of each patient, the iris was brought into view using the mouse-driven alignment system, and the ophthalmoscopic image was focused. Automated measurements of the peripapillary and macular choroid were recorded using a 360° 6-mm diameter circle. The choroid analysis algorithm processed data from 3D volume scans with measured thicknesses of the macular and peripapillary choroid. Choroidal thickness was measured across eight sectors for both the macular and peripapillary choroid. Subfoveal choroidal thickness was measured from centring the elliptical annulus on the fovea (Fig. 1a, b). Mean thickness values for each layer were calculated for the topographical retinal areas of the standard grid template centred at the fovea. This included the central 1 mm region along with the four quadrants of the inner annular ring (1–3 mm radius), and the four quadrants of the outer annular ring (3–6 mm radius) (Fig. 1c, d). RNFL and RGC-IPL thicknesses were measured using a 360° 3.4-mm diameter circle scan with thicknesses measured across the superior, nasal, inferior, and temporal sectors. All images were acquired by an experienced operator. The built-in SS-OCT eye-tracking system was used to provide reproducible measurements. The quality of each scan and accuracy of the segmentation algorithm were reviewed by an experienced, blinded examiner. Images with segmentation failures, significant motion artefacts, or signal strength less than 6 were excluded.

Statistical methods

Statistical analysis was performed using the Statistical Package for Social Sciences (version 21 SPSS Inc. Chicago, IL, USA). A Shapiro–Wilk test was used to evaluate the
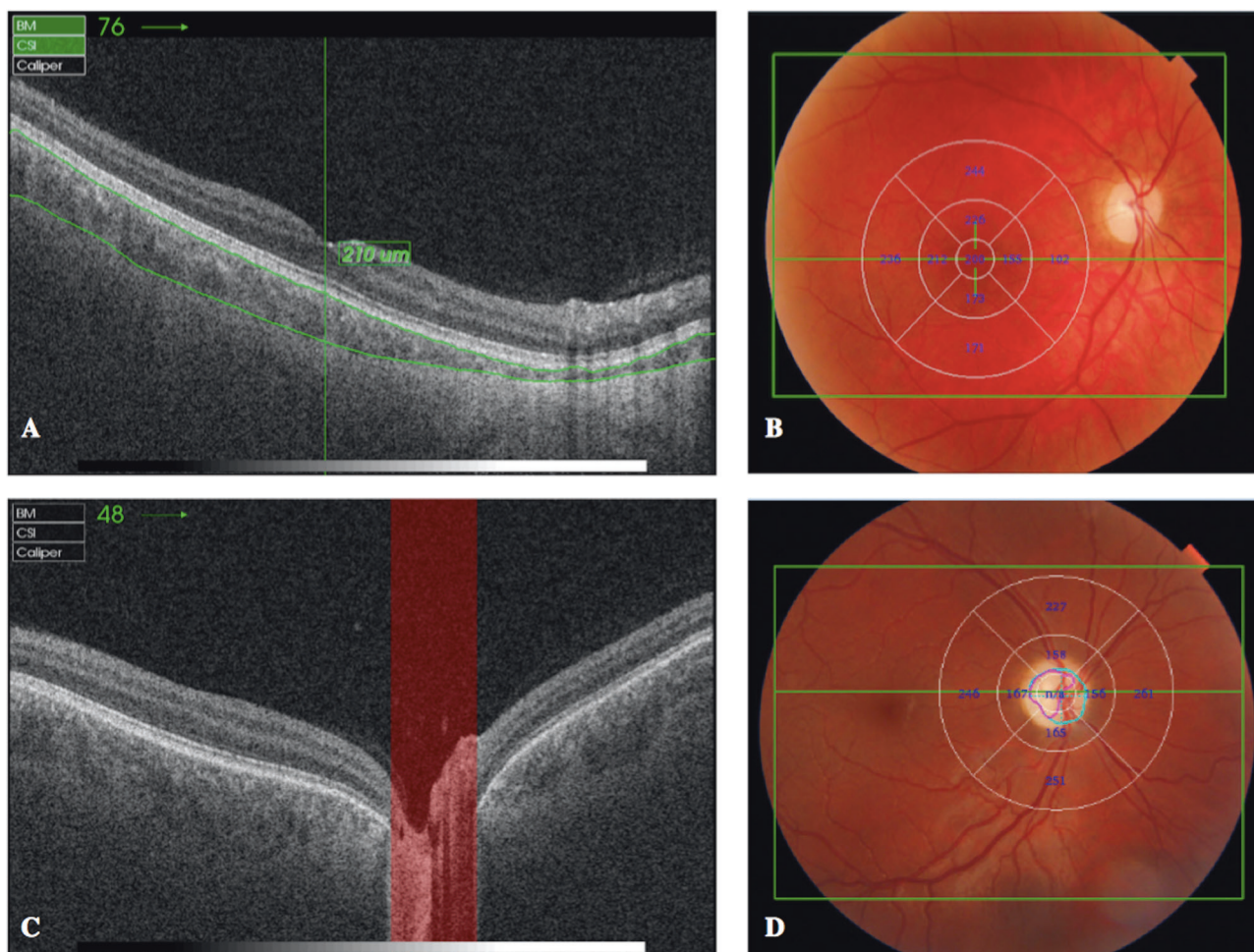
Fig. 1 Imaging of choroidal thickness for the macular and peripapillary regions using swept-source optical coherence tomography (SS-OCT). **a** Representative OCT B-scan with **b** corresponding 360°, 6 mm diameter circle scan centred on the fovea, from a healthy subject (control group). **c** Representative OCT B-scan with **d** corresponding 360°, 6 mm diameter circle scan centred on the optic disk, from a healthy subject (control group)

normal distribution of the variables. All variables were reported as a mean ± standard deviation and compared using one-way analysis of covariance, including age and gender as covariates. Given the data did not follow a normal distribution, a non-parametric Mann–Whitney U test (independent Student's t test) was performed for pair-wise comparisons. Pearson correlation was performed between choroidal thickness and RGCL or RNFL thickness. Statistical significance was selected at a $p < 0.05$.

Results

Demographic data

Table 1 shows the demographic data of chronic LHON patients and healthy controls. One eye from the LHON group and two eyes from the age-matched control group were excluded from analysis due to poor scan quality.

Table 1 Study participants' demographic and clinical features

	Chronic LHON	Healthy controls
Number of participants (number of eyes)	26 (26)	27 (27)
Gender (number of males)	21	19
Number of smokers	0	0
Age, years	35.1 ± 16.0	32.4 ± 11.1 ($p = 0.45$)
Disease duration, years	4.5 ± 2.5	–
Visual acuity, logMAR	1.6 ± 0.8	0

Data are shown as mean ± SD

RNFL and RGC-IPL

Mean total RNFL thickness was $50.4 \pm 17.8\ \mu m$ in chronic LHON patients and $111.3 \pm 11.8\ \mu m$ in control patients ($p < 0.005$). Mean total RGCL thickness was $43.0 \pm 7.1\ \mu m$

Table 2 Comparison of macular choroidal thickness between LHON patients and controls as measured by swept-source OCT

Sector	Chronic LHON	Healthy Controls	Difference	p value
Subfoveal	262.7 ± 73.9	334 ± 71.7	-71.3 ± 15.9	$p < 0.0001$
IS	260.8 ± 72.1	332.4 ± 67.1	-71.6 ± 15.2	$p < 0.0001$
IN	248.9 ± 67.4	308.1 ± 73.1	-59.2 ± 15.4	$p < 0.0001$
II	264.3 ± 74.6	323.1 ± 69.2	-58.8 ± 15.9	$p < 0.0001$
IT	259.0 ± 70.6	325.9 ± 63.5	-66.9 ± 14.6	$p < 0.0001$
OS	258.0 ± 73.3	324.6 ± 64.6	-66.6 ± 15.1	$p < 0.0001$
ON	195.9 ± 61.8	259.2 ± 68.9	-63.3 ± 14.3	$p < 0.0001$
OI	254.7 ± 69.4	313.2 ± 75.2	-58.6 ± 15.8	$p < 0.0001$
OT	250.4 ± 64.3	304.4 ± 59.1	-54.0 ± 13.5	$p < 0.0001$
Average	250.5 ± 62.2	313.9 ± 60.2	-63.4 ± 13.3	$p < 0.0001$

Data are shown as mean ± SD

IS inner superior, *IN* inner nasal, *II* inner inferior, *IT* inner temporal, *OS* outer superior, *ON* outer nasal, *OI* outer inferior, *OT* outer temporal

in chronic LHON patients and 86.0 ± 4.1 μm in control patients ($p < 0.005$). RNFL and RGC-IPL sectoral analyses are shown in the Supplementary material.

Choroidal analyses

The macular choroid was markedly thinner in LHON relative to controls across all measured sectors. As seen in Table 2, thinning was most pronounced in the subfoveal and inner superior regions and least pronounced in the outer temporal region. Similarly, the peripapillary choroid was significantly thinner in LHON relative to controls across all measured sectors. As seen in Table 3, thinning was most pronounced in the superior sector and least pronounced in the nasal sector.

Pearson correlation testing for the average measurements of the RNFL and the choroid showed a shared pattern of thinning in LHON, which was more apparent in the macular region (Fig. 2a: $R^2 = 0.72$; 95% CI, 0.57–0.84) than in the peripapillary region (Fig. 2b: $R^2 = 0.53$; 95% CI, 0.31–0.70). The RGC-IPL was also significantly correlated with the choroid, although specifically within the macular region (Fig. 2c: $R^2 = 0.51$; 95% CI, 0.26–0.73). The RGC-IPL and the peripapillary choroid were weakly correlated (Fig. 2d: $R^2 = 0.34$; 95% CI, 0.10–0.55).

Discussion

Our group recently showed a direct in vivo correlation between RNFL and choroidal thickness in both the macular and peripapillary regions using an SD-OCT device [11]. The current prospective study uses an SS-OCT device to quantitatively investigate and compare both RNFL and RGC-IPL thickness profiles with that of the choroid in patients with chronic LHON mtDNA 11778. We expand

Table 3 Comparison of peripapillary choroidal thickness between LHON patients and controls as measured by swept-source OCT

Sector	Chronic LHON	Healthy controls	Difference	p value
IS	105.4 ± 62.3	164.6 ± 73.0	-59.2 ± 14.8	$p < 0.0001$
IN	107.2 ± 55.0	134.6 ± 58.22	-27.4 ± 12.4	$p < 0.006$
II	100.8 ± 44.8	149.3 ± 74.6	-48.5 ± 13.5	$p < 0.0001$
IT	113.8 ± 54.2	160.4 ± 68.5	-46.6 ± 13.5	$p < 0.0001$
OS	172.6 ± 61.3	232.3 ± 62.2	-59.7 ± 13.5	$p < 0.0001$
ON	161.2 ± 57.0	196.3 ± 48.8	-35.1 ± 11.6	$p < 0.02$
OI	139.8 ± 51.1	187.69 ± 74.6	-47.9 ± 14.0	$p < 0.001$
OT	184.7 ± 62.3	239 ± 71.2	-54.3 ± 14.6	$p < 0.01$
Average	135.7 ± 51.4	183.01 ± 61.8	-47.4 ± 12.4	$p < 0.0007$

Data are shown as mean ± SD

IS inner superior, *IN* inner nasal, *II* inner inferior, *IT* inner temporal, *OS* outer superior, *ON* outer nasal, *OI* outer inferior, *OT* outer temporal

upon our previous work by demonstrating that, in addition to the RNFL, choroidal thinning is accompanied by, and directly correlated with, RGC-IPL thinning.

The RNFL and the choroid were both significantly thinner and directly correlated in LHON patients. This is consistent with our previous study, which showed that RNFL thinning likely starts earlier relative to the choroid, and that the two entities are directly correlated over the course of the disease [11]. We found that RNFL thickness directly correlated with both the macular and peripapillary choroid, and this correlation was more significant in the macular region. This further supports our proposed theory of continual axonal loss in LHON over time [12]. Our laboratory and others have previously shown that in LHON, mtDNA point mutations affecting Complex I of the mitochondrial respiratory chain impair electron transfer in oxidative phosphorylation. This impairment leads to decreased energy or ATP production and consequent reactive oxygen
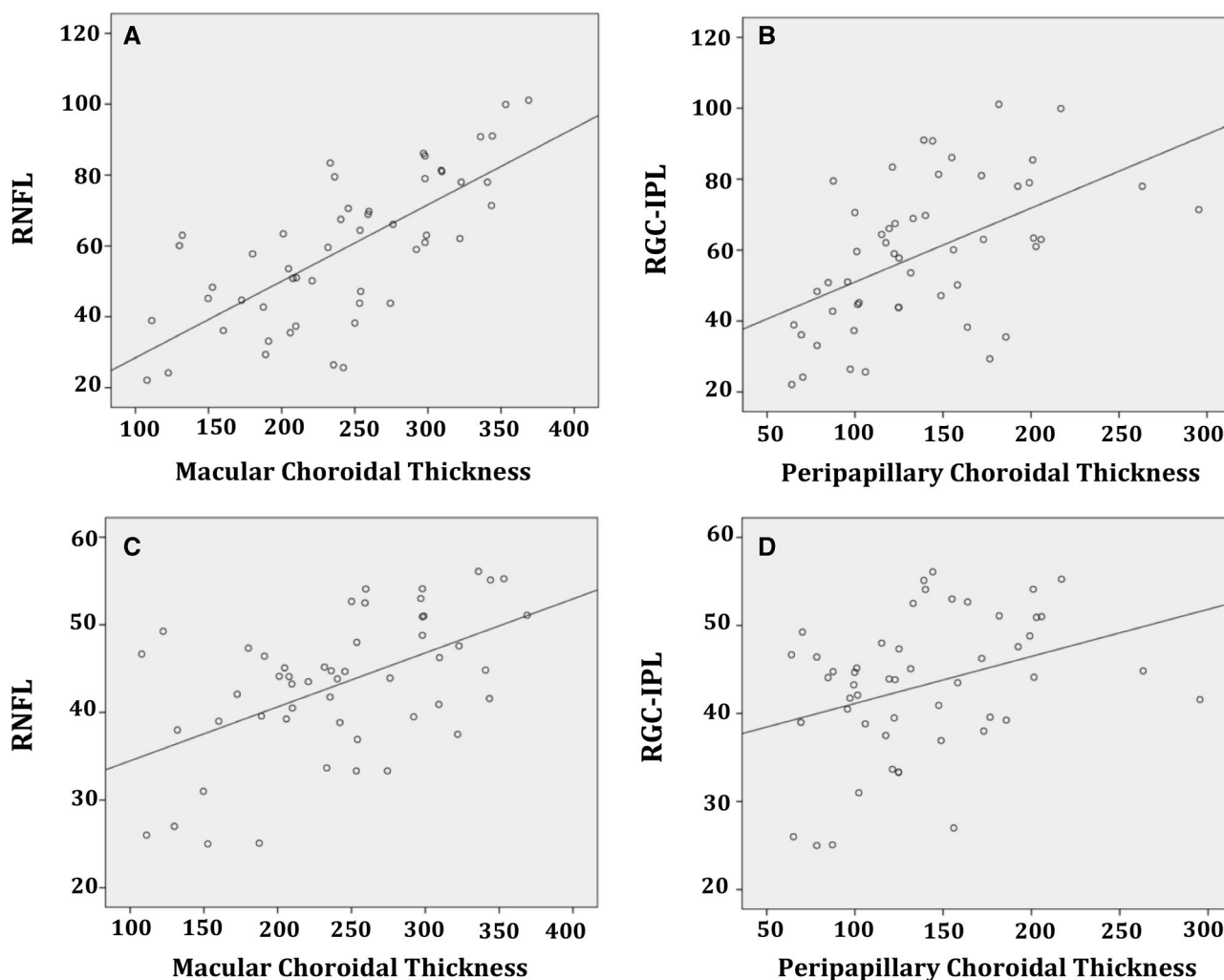
Fig. 2 Pearson correlation tests between: **a** retinal nerve fibre layer (RNFL) and macular choroid thickness, and **b** RNFL and peripapillary choroidal thickness in chronic LHON patients. **c** Retinal ganglion cell-inner plexiform layer (RGC-IPL) and macular choroid thickness. **d** RGC-IPL and peripapillary choroidal thickness in chronic LHON patients

species (ROS) overproduction [12–15, 17, 18]. Studies conducted by Bonello et al. have demonstrated that ROS directly link hypoxia inducible factor 1 (HIF-1)-alpha and nuclear factor kappa light chain enhancer of activated B cells (NF-kappaB), suggesting the importance of this pathway in disorders associated with elevated levels of ROS such as LHON [19]. Given these findings, we propose that the overproduction of ROS seen with axonal degeneration in LHON may promote the signalling of angiogenic factors and contribute to vascular changes of the choroid. Specifically, a low rate of ongoing axonal degeneration and overproduction of ROS likely continues vascular signalling, which may explain the prolonged choroidal remodelling seen in chronic LHON [11–15, 17–19]. This is surprising in the peripapillary region insofar as the RNFL is inner retina and the choroid supplies the outer retina. Alternatively, but less likely, there was an additional vascular pathology that paralleled events in the inner retina.

The current study also assessed RGC-IPL thickness in relation to the choroid. We found that the RGC-IPL was both significantly thinner and directly correlated with choroidal thickness in LHON patients. Similar to the RNFL, RGC-IPL thickness was more closely correlated with choroidal thickness in the macular region relative to the peripapillary region. Balducci et al. recently showed that macular RGC-IPL thickness changes likely precede the wave of peripapillary RNFL swelling in acute LHON [20, 21]. Taken together, our findings suggest that a similar sequence of events continues to occur even in chronic LHON. In particular, choroidal thinning possibly begins in the macular region and is later followed by thinning in the peripapillary region. This notion may likely explain the greater thickness reduction exhibited in the macular choroid relative to the peripapillary choroid in chronic LHON. Alternatively, the central macula, not only having a retinal blood supply, is more dependent on the choroid.

Vascular changes including transient peripapillary microangiopathy and telangiectasias have been well characterized in LHON. However, these features are hallmarks primarily seen in acute stages of LHON [9–11]. In chronic stages of LHON, our laboratory recently showed significant vascular attenuation in the macula using OCT angiography (OCTA) [22]. Using OCTA in chronic LHON, Borrelli et al. observed a decrease in retinal perfusion that was most pronounced in areas of extensive neuronal damage [22]. Previous studies have described a coupling between blood supply and the energy demands of the retina such that blood flow is regulated towards functionally active areas of the retina and diverted away from inactive or damaged areas of the retina [23–25]. This pairing of blood supply and retinal metabolism may explain Borrelli et al. findings in chronic LHON whereby extensive neuronal damage in the retina may be associated with a reduced metabolic demand and a corresponding reduction in retinal perfusion [22–25]. Intriguingly, our results demonstrated that the greater choroidal thickness reduction seen in the macular region was topographically associated with the region occupied by the papillomacular bundle, which is where mitochondrial dysfunction and ganglion cell loss first occur in LHON [11, 26–30]. Studies have shown that the overproduction of ROS from complex I deficiency in LHON leads to the upregulation of trophic factors as similarly seen in hypoxic ischaemic conditions [12, 15, 18, 19, 31]. Therefore, choroidal thickness changes in LHON may represent mitochondrial angiopathy involving angiogenic trophic factors as a compensatory response to a "pseudo-hypoxic" state perhaps mediated by ROS [11, 15, 18, 19, 28, 31]. Given a reduced metabolic demand of the macula in chronic LHON, as previously suggested [22–25], a greater thickness reduction for the macular choroid was expected and observed in our study. Since we exclusively assessed chronic LHON patients exhibiting an advanced loss of macular ganglion cells, the significant correlation with the choroid further supports a vascular aetiology involved in the complex pathophysiology of this disorder.

Conclusions and future directions

The current study provides clues to a more complete understanding of LHON mechanisms in relation to vascular pathology. We used SS-OCT to assess the choroid at a greater resolution and depth compared with previous studies using SD-OCT. In addition, choroidal thickness measurements were acquired in an automated fashion with reliable repeatability. Morphological assessment of the choroid using SS-OCT may offer certain clinical advantages given vascular abnormalities are not only observed in asymptomatic LHON carriers, but also are associated with an increased risk of converting to the disease state [8–10]. The current results may be used as a basis for future studies evaluating the natural disease course. Nevertheless, additional studies of choroidal vascular measures in conjunction with RGC-IPL measurements are warranted to demonstrate their utility as useful biomarkers for monitoring the efficacy of purported therapies in patients with LHON. Since this prospective study was exploratory and cross-sectional in nature, a power calculation was not performed and proper characterization of LHON natural history requires a long-term longitudinal follow-up study. Future studies may benefit from investigating correlations between structure and function to further support choroidal thinning as an important measure of treatment effect.

Summary

What was known before

- Choroidal thinning has been suggested in LHON.
- This thinning may be related to the neural retina. However, choroidal thinning in relation to the RGC-IPL has not previously been studied.

What this study adds

- Choroidal thickness correlates strongly with both RNFL and RGC-IPL thicknesses in chronic disease.
- Vascular pathology may be involved in LHON pathophysiology.

Compliance with ethical standards

References

1. Leber T. About hereditary and congenital optic nerve disorders. Albrect Von Graefes Arch Clin Exp Ophthalmol. 1871;17: 249–91.
2. Yu-Wai-Man P, Griffiths PG, Chinnery PF. Mitochondrial optic neuropathies – disease mechanisms and therapeutic strategies. Prog Retin Eye Res. 2011;30:81–114.
3. Newman NJ. Hereditary optic neuropathies: from the mitochondria to the optic nerve. Am J Ophthalmol. 2005;140:517–23.

4. Mackey DA, Oostra RJ, Rosenberg T, Nikoskelainen E, Bronte-Stewart J. Primary pathogenic mtDNA mutations in multigeneration pedigrees with Leber hereditary optic neuropathy. Am J Hum Genet. 1996;59:481–5.

5. Barboni P, Carbonelli M, Savini G, Ramos Cdo V, Carta A, Berezovsky A, et al. Natural history of Leber's hereditary optic neuropathy: longitudinal analysis of the retinal nerve fiber layer by optical coherence tomography. Ophthalmology. 2010;117:623–7.

6. Barboni P, Savini G, Valentino ML, Montagna P, Cortelli P, De Negri AM, et al. Retinal nerve fiber layer evaluation by optical coherence tomography in Leber's hereditary optic neuropathy. Ophthalmology. 2005;112:120–6.

7. Nikoskelainen EK, Huoponen K, Juvonen V, Lamminen T, Nummelin K, Savontaus ML. Ophthalmologic findings in Leber hereditary optic neuropathy, with special reference to mtDNA mutations. Ophthalmology. 1996;103:504–14.

8. Nikoskelainen E, Hoyt WF, Nummelin K. Ophthalmoscopic findings in Leber's hereditary optic neuropathy. I. Fundus findings in asymptomatic family members. Arch Ophthalmol. 1982; 100:1597–602.

9. Nikoskelainen E, Hoyt WF, Nummelin K. Ophthalmoscopic findings in Leber's hereditary optic neuropathy: II. The fundus findings in the affected family members. Arch Ophthalmol. 1983; 101:1059–68.

10. Nikoskelainen E, Nummelin K, Hoyt WF, Schatz H. Fundus findings in Leber's hereditary optic neuroretinopathy III. Fluorescein angiographic studies. Arch Ophthalmol. 1984;102:981–9.

11. Borrelli E, Triolo G, Cascavilla ML, La Morgia C, Rizzo G, Savini G, et al. Changes in choroidal thickness follow the RNFL changes in Leber's hereditary optic neuropathy. Sci Rep. 2016;6:37332.

12. Carelli V, Ross-Cisneros FN, Sadun AA. Mitochondrial dysfunction as a cause of optic neuropathies. Prog Retin Eye Res. 2004;23:53–89.

13. Sadun AA. Mitochondrial optic neuropathies. J Neurol Neurosurg Psychiatry. 2002;72:423–5.

14. Carelli V, La Morgia C, Iommarini L, Carroccia R, Mattiazzi M, Sangiorg S, et al. Mitochondrial optic neuropathies: how two genomes may kill the same cell type? Biosci Rep. 2007;27:173–84.

15. Chevrollier A, Guillet V, Loiseau D, Gueguen N, de Crescenzo MA, Verny C, et al. Hereditary optic neuropathies share a common mitochondrial coupling defect. Ann Neurol. 2008;63:794–8.

16. Dastiridou AI, Bousquet E, Kuehlewein L, Tepelus T, Monnet D, Salah S, et al. Choroidal imaging with swept-source optical coherence tomography in patients with birdshot chorioretinopathy: choroidal reflectivity and thickness. Ophthalmology. 2017;124:1186–95.

17. Carelli V, La morgiaC, Valentino ML, Barboni P, Ross-cisneros FN, Sadun AA. Retinal ganglion cell neurodegeneration in mitochondrial inherited disorders. Biochim Biophys Acta. 2009; 1787:518–28.

18. Sadun AA, Carelli V, La Morgia C, Karanjia R. Leber's hereditary optic neuropathy (LHON) mtDNA mutations cause cell death by overproduction of reactive oxygen species. Acta Ophthalmol. 2015;93:S255.

19. Bonello S, Zähringer C, BelAiba RS, Djordjevic T, Hess J, Michiels C, et al. Reactive oxygen species activate the HIF-1alpha promoter via a functional NFkappaB site. Arterioscler Thromb Vasc Biol. 2007;27:755–61.

20. Balducci N, Savini G, Cascavilla ML, La Morgia C, Triolo G, Giglio R, et al. Macular nerve fibre and ganglion cell layer changes in acute Leber's hereditary optic neuropathy. Br J Ophthalmol. 2016;100:1232–7.

21. Jurkute N, Yu-wai-man P. Leber hereditary optic neuropathy: bridging the translational gap. Curr Opin Ophthalmol. 2017;28:403–9.

22. Borrelli E, Balasubramanian S, Triolo G, Barboni P, Sadda SR, Sadun AA. Topographic macular microvascular changes and correlation with visual loss in chronic leber hereditary optic neuropathy. Am J Ophthalmol. 2018;192:217–28.

23. Wong-Riley M. Energy metabolism of the visual system. Eye Brain. 2010;2:99–116.

24. Yu DY, Yu PK, Cringle SJ, Kang MH, Su EN. Functional and morphological characteristics of the retinal and choroidal vasculature. Prog Retin Eye Res. 2014;40:53–93.

25. Yu DY, Cringle SJ, Yu PK, Balaratnasingam C, Mehnert A, Sarunic M, et al. Retinal capillary perfusion: spatial and temporal heterogeneity. Prog Retin Eye Res. 2019;70:23–54.

26. Giles RE, Blanc H, Cann HM, Wallace DC. Maternal inheritance of human mitochondrial DNA. Proc Natl Acad Sci USA. 1980; 77:6715–9.

27. Wallace D, Singh G, Lott M, Hodge JA, Schurr TG, Lezza AM, et al. Mitochondrial DNA mutation associated with Leber's hereditary optic neuropathy. Science. 1988;242:1427–30.

28. Sadun AA, La Morgia C, Carelli V. Mitochondrial optic neuropathies: our travels from bench to bedside and back again. Clin Exp Ophthalmol. 2013;41:702–12.

29. Pan BX, Ross-Cisneros FN, Carelli V, Rue KS, Salomao SR, Moraes-Filho MN, et al. Mathematically modeling the involvement of axons in Leber's hereditary optic neuropathy. Investig Ophthalmol Vis Sci. 2012;53:7608–17.

30. Borrelli E, Lonngi M, Balasubramanian S, Tepelus TC, Baghdasaryan E, Iafe NA, et al. Macular microvascular networks in healthy pediatric subjects. Retina. 2018;39:1216–24.

31. Jain IH, Zazzeron L, Goli R, Alexa K, Schatzman-Bone S, Dhillon H, et al. Hypoxia as a therapy for mitochondrial disease. Science. 2016;352:54–61.